Desalination and Water Treatment
www.deswater.com

doi: 10.5004/dwt.2021.26899

217 (2021) 253–261
March

Precipitation of cadmium in water by the addition of phosphate solutions prepared from digested samples of waste animal bones

Sonia Jebri[a,*], Mouna Jaouadi[b], Ismail Khattech[c]

[a]*Natural Water Treatment Laboratory, Water Researches and Technologies Center, Technologic Park of Borj Cedria, B.P. 273, Soliman 8020, Tunisia, email: Sonia.jebri@gmail.com*
[b]*Useful Materials Valorization Laboratory, National Center of Research in Materials Science, Technologic Park of Borj Cedria, B.P. 73, Soliman 8020, Tunisia, email: ing.mouna@gmail.com*
[c]*Materials Cristal Chemistry and Applied Thermodynamics Laboratory, Faculty of Science, Chemistry Department, LR15SE01, Université de Tunis El Manar, Tunis 2092, Tunisia, email: ismail.khattech@fst.utm.tn*

Received 3 July 2020; Accepted 27 November 2020

ABSTRACT

Chemical neutralization of aqueous cadmium by adding soluble phosphorus compounds has been successfully applied to treat contaminated waters. However, the reagent costs are relatively high. The present work proposes a novel alternative approach for removing aqueous cadmium from wastewaters through an *in-situ* precipitation reaction promoted by adding phosphate solutions prepared by acid digestion of waste animal bones. As the major components of the biologic phosphates, calcium hydroxyapatite $Ca_{10}(PO_4)_6(OH)_2$, and tricalcium phosphate $Ca_3(PO_4)_2$ powders were firstly synthesized and used as model sources of PO_4^{-3} ions to investigate the optimal neutralization conditions. The extraction at pH 7 revealed that equilibrium was rapidly established, and the kinetics data could well be described by the pseudo-second-order model. This model is related to chemical bonding reactions between Cd^{2+} from synthetic wastewater with a Cd^{2+} concentration of 50 mg L^{-1} and the added bone-derived ions (Ca^{2+}, PO_4^{-3}), forming $Ca_{(10-x)}$-Cd_x-phosphate apatites with Cd molar fractions x up to ~8.7. The precipitates were characterized by different spectroscopic techniques (Fourier transform infrared, X-ray diffraction, and scanning electron microscopy-energy dispersive X-ray spectroscopy). The experiments revealed that this novel approach enables removing high degrees (up to ~99%) of aqueous cadmium from contaminated waters with Cd^{2+} concentrations within the range of 50-500 mg L^{-1}.

Keywords: Cadmium; Precipitation; Phosphate solutions; Waste animal bones; Wastewater

1. Introduction

Contamination due to the presence of heavy metals in soil, surface, and groundwater, is one of the major issues of the environmental sciences. The main sources of metals released into the environment include industrial wastes, operating mining sites, phosphate fertilizer manufacture, and use [1–3]. Nowadays, much attention is being paid to the environmental problems associated with heavy metals. Thus, there are considerable scientific and technological interests in modeling the environmental flow of aqueous metals, and in implementing effective regulatory control strategies to mitigate these problems.

One of the most harmful heavy metals, even at a low level, is cadmium [4–6]. The most severe stage of chronic poisoning related to cadmium exposure by oral route is the Itai–Itai disease, described in Japan in the 1960s [7]. Its bioaccumulation in human organisms could degenerate

---

* Corresponding author.

into very serious diseases such as kidney dis-function [8], hypertension [9], osteoporosis [10], and even cancer [11,12]. Therefore, continuous efforts have been made toward reducing this pollutant from contaminated sites. With this purpose, several methods have been attempted such as precipitation [13,14], membrane separation [15], ion exchange [16], biological process [17], and adsorption on activated carbon and apatites [18–20]. Among these remediation techniques, the *in-situ* phosphate formation is potentially the most environmentally attractive one due its ability to immobilize high levels of toxic metals into stable phosphate compounds, such as tricalcium phosphate $Ca_3(PO_4)_2$ (TCP) and calcium hydroxyapatite $Ca_{10}(PO_4)_6(OH)_2$ (HAp), with heavy metal cations partially replacing Ca^{2+} ions in their lattices. Such replacements are facilitated especially when the ionic species have similar ionic radii as in the case Cd^{2+} (0.95 Å) and Ca^{2+} (1.00 Å). However, the ability of calcium phosphates to accommodate strange ionic species with significantly different ionic radii such as Sr^{2+} (1.20 Å), Mg^{2+} (0.69 Å), and Zn^{2+} (0.74 Å) [21–26], and many other, including anions [26], has been intensively explored for incorporating therapeutic ions and obtaining biomaterials with enhanced biological performances.

Cadmium, like other heavy metals in water, could be neutralized by its adsorption onto calcium phosphates through batch equilibrium technique [27,28], or by precipitation of metal-phosphates through the addition of the soluble phosphorus compounds [13]. Thereby, the mobile ionic forms are converted into stable metal-phosphates, alleviating the environmental concerns [29]. Nevertheless, the manufacturing costs of sorbents and the relatively high expensive chemicals used to precipitate this pollutant constitute the main drawbacks of these procedures.

The novel alternative approach adopted in the present study involves the acid digestion of waste animal bones and using the as obtained phosphate-containing solution to precipitate aqueous cadmium from contaminated waters. The efficacy of the procedure was firstly tested using acid solutions of synthetic HAp and TCP powders with different concentrations as sources of PO_4^{3-} ions, since these calcium phosphate phases are the major components of the biological phosphates [25,26,30]. The optimal precipitation/neutralization conditions were then applied to the P-containing solutions derived from the acid digestion of waste animal bones.

2. Materials and methods

2.1. Material preparation and characterization

Samples of rabbit and chicken waste bones were collected from local restaurants, separated by animal type, and hereafter denoted as RBw and CBw, respectively. The samples were firstly cleaned and boiled in water for 2 h in order to facilitate the removal of soft tissues and collagen. After that, the defatted samples were dried and finely grinded to powders, and finally submitted to acid digestion without any further thermal treatment. Energy-dispersive X-ray spectroscopy (EDS) analyses were carried out on the powdered bones in order to determine the main elements. According to the chemical analysis, the compositions of the biological apatites can be expressed by the following formulas:

$$\text{RBw: } Ca_{9.62}Mg_{0.14}Na_{0.19}Al_{0.04}(PO_4)_{5.62}(CO_3)_{0.38}(OH)_{1.62} \quad (1)$$

$$\text{CBw: } Ca_{9.42}Mg_{0.25}Na_{0.23}Al_{0.10}(PO_4)_{5.42}(CO_3)_{0.58}(OH)_{1.42} \quad (2)$$

The model phosphate compounds were synthesized according to the wet precipitation route [31,32]. Thus, HAp powder was prepared by the dropwise addition of a diammonium hydrogen phosphate solution $(NH_4)_2HPO_4$ into a boiling solution of calcium nitrate $Ca(NO_3)_2{\cdot}4H_2O$, whereas, TCP powder was obtained by the fast precipitation technique which consists in quickly pouring the first solution into the second one at room temperature. The stoichiometric calcium to phosphorous molar ratios were planned, (Ca/P = 1.67 for HAp, and Ca/P = 1.50 for TCP). The synthesis of these compounds could be described by the following schemes:

$$10Ca(NO_3)_2 + 6(NH_4)_2HPO_4 + 8NH_4OH \rightarrow Ca_{10}(PO_4)_6(OH)_2 + 20NH_4NO_3 + 6H_2O \quad (3)$$

$$9Ca(NO_3)_2 + 6(NH_4)_2HPO_4 + 6NH_4OH \rightarrow 3Ca_3(PO_4)_2 + 18NH_4NO_3 + 6H_2O \quad (4)$$

The powders were characterized by X-ray diffraction (XRD) and Fourier transform infrared (FTIR) spectroscopy, as reported elsewhere [31,32]. The lattice parameters determined for both samples allowed us to certify the purity of these products. Moreover, FTIR spectrum of HAp, exhibited the characteristic absorbance bands of PO_4^{3-} groups appearing at 567; 601; 962; 1,039; and 1,090 cm^{-1}. The bands centered at 630 and 3,570 cm^{-1} were assigned to the structural OH^- groups. On the other hand, the recorded spectrum for TCP sample revealed only the characteristic absorbance bands of PO_4^{3-} groups located in the region 551–1,103 cm^{-1}. All these minerals were submitted to acid digestion as described in the next section.

2.2. Preparation of phosphate solutions

The phosphate solutions derived from the synthesized model compounds (S_{HAp} and S_{TCP}) were prepared by dissolving 1 g of each powder in 8 mL of a 6 wt.% HNO_3 solution. The liquid was kept under vigorous stirring and the total volume was adjusted to 50 mL with distillate water. A similar procedure was adopted for preparing the phosphate solutions derived from the animal waste bones (S_{RBw} and S_{CBw}), but the concentration of the HNO_3 solution used for acid digestion was increased to 12 wt.%.

2.3. Cadmium neutralization technique

The cadmium neutralization procedure consisted in adding 0.25–7 mL of the as prepared phosphate solutions into 100 mL of the metal-contaminated waters with various initial concentrations. The starting pH of the reaction medium was adjusted to three different: 5.0 ± 0.2, 7.0 ± 0.2, and 9.0 ± 0.2 by adding sodium hydroxide (0.1–1 M) solutions and no further attempts were made to maintain this parameter constant during the experiments. The precipitated white Ca-Cd-phosphate apatites were kept under continuous stirring for 1 h to provide homogeneity, and the as obtained suspensions were vacuum filtrated. The powders were dried at 70°C and characterized by spectroscopic techniques, whereas the filtrate was analyzed for the residual Cd^{2+} content. The neutralization rate of Cd^{2+} ions (%) in the treated water was evaluated from the change in the solution's concentration, Eq. (5):

$$\text{Neutralization rate}\left(\%\right)=\frac{\left(C_0-C_e\right)}{C_0}\times 100 \qquad (5)$$

where C_0 and C_e (mg L^{-1}) are the concentrations of Cd^{2+} ions in the liquid phase before and after the extraction. An overview of the described procedure is illustrated in Fig. 1. The experiments were performed in duplicate and the error on the measurement was found to be less than 5%. On the other hand, the Cd^{2+} solutions with various concentrations were prepared by diluting a stock solution of cadmium nitrate at initial metal concentration 1,000 mg L^{-1}.

Assuming the formation of monophasic compounds of Ca-Cd-phosphates under alkaline pH conditions, Cd^{2+} ions will be precipitated according to the following reactions:

$$(10-x)\text{Ca}^{2+}_{(\text{sol})} + 6\text{PO}^{3-}_{4(\text{sol})} + 2\text{OH}^{-}_{(\text{sol})} + x\text{Cd}^{2+}_{(\text{sol})} \xrightarrow{\text{pH}>7} \text{Ca}_{(10-x)}\text{Cd}_x\left(\text{PO}_4\right)_6\left(\text{OH}\right)_{2(\text{s})} \qquad (6)$$

$$(3-x)\text{Ca}^{2+}_{(\text{sol})} + 2\text{PO}^{3-}_{4(\text{sol})} + x\text{Cd}^{2+}_{(\text{sol})} \xrightarrow{\text{pH}>7} \text{Ca}_{(3-x)}\text{Cd}_x\left(\text{PO}_4\right)_{2(\text{s})} \qquad (7)$$

where x is the molar fraction of cadmium into the continuous solid solution of Ca-Cd-phosphate ($0 \leq x \leq 10$ for HAp and $0 \leq x \leq 3$ for TCP) [33,34]. This parameter could be evaluated from the following expression:

$$x=\frac{n_{\text{Cd}}}{n_{\text{Ca-phosphate}}}=\frac{\left(C_0-C_e\right)V_{\text{Cd}}}{20V_{\text{add}}}\frac{M_{\text{Ca-phosphate}}}{M_{\text{Cd}}} \qquad (8)$$

where V_{Cd} is the volume of the metal solution (L), V_{add} is the added volume of S_{HAp} or S_{TCP} (mL), $n_{\text{Ca-phosphate}}$ is the molar content of the testing solution, M_{Cd} and $M_{\text{Ca-phosphate}}$ are the atomic weights of cadmium and the dissolved starting calcium phosphate, respectively (g mol^{-1}).

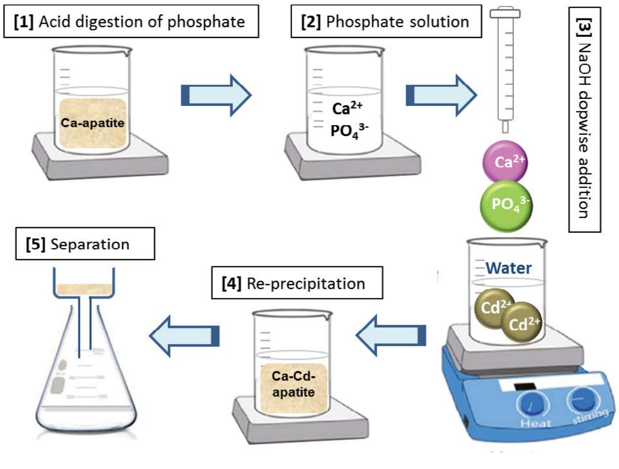

Fig. 1. Schematic illustration of Cd^{2+} neutralization in Cd-contaminated water through acid digestion of animal waste bones and NaOH-assisted precipitation of Ca–Cd–phosphate apatites.

2.4. Analytical methods

The identification of the crystalline phases was carried out by XRD technique. The measurements were made with a D8 ADVANCE Bruker diffractometer (Germany) using copper radiations ($K\alpha_1$ = 1.5406 Å; $K\alpha_2$ = 1.5445 Å). Attenuated total reflectance-Fourier transform infrared spectroscopy (ATR-FTIR) was applied to identify the functional groups of the different phosphates. The spectra were recorded between 400 and 4,000 cm^{-1} using a PerkinElmer Spectrum 100 FTIR spectrometer (USA). The morphological modifications of the natural apatites after being re-precipitated in Cd-loaded solutions were observed by ultra-high-resolution Analytical Electron Microscope HR-FESEM Hitachi SU-70 (Japan) field emission scanning electron microscopy (FESEM) coupled to EDS system for elemental analyses (SEM-EDS). The Cd^{2+} contents remaining in the treated water were determined by means a flame atomic absorption Spectrometer novAA 350 Analytik Jena (Germany).

3. Results and discussion

3.1. Modeling of Cd^{2+} precipitation

3.1.1. Effect of the phosphate solution dose on the cadmium removal efficiency

In order to determine the most suitable experimental conditions leading to the highest neutralization rates, series of experiments were carried out on Cd^{2+} solutions by varying both the initial metal concentrations (from 10 to 50 mg L^{-1}) and the volumes of the added phosphate S_{HAp} and S_{TCP} solutions (from 0.25 to 7 mL). The results for Cd^{2+} precipitation as Ca-Cd-phosphate apatite solid solutions at pH 7 are displayed in Fig. 2.

In general, the precipitated quantities of Cd^{2+} ions are sensibly increased up to 2 mL of the added phosphate solution (S_{HAp}) and 1 mL of its homologous (S_{TCP}). The results also show that the removal extent is greatly influenced by the initial metal concentration. In fact, increasing this parameter from 10 to 50 mg L^{-1}, increases the neutralization rate from 65% to 95% upon adding S_{HAp}, and from 50% to 99% by the addition of S_{TCP}, while the optimal added volume decreased to 0.25 mL for both solutions.

3.1.2. Effect of the initial cadmium concentration on its removal efficiency

The incorporated amounts of cadmium per unit cell of $\text{Ca}_{(10-x)}\text{Cd}_x(\text{PO}_4)_6(\text{OH})_2$ and $\text{Ca}_{(3-x)}\text{Cd}_x(\text{PO}_4)_2$ compounds were determined for the different initial metal concentrations. The results obtained are listed in Table 1. It should be noticed that the method seems to be particularly interesting for initial metal concentrations exceeding 30 mg L^{-1} as indicated by the evolution of x parameter against C_0. Indeed, the availability of a reactant generally increases

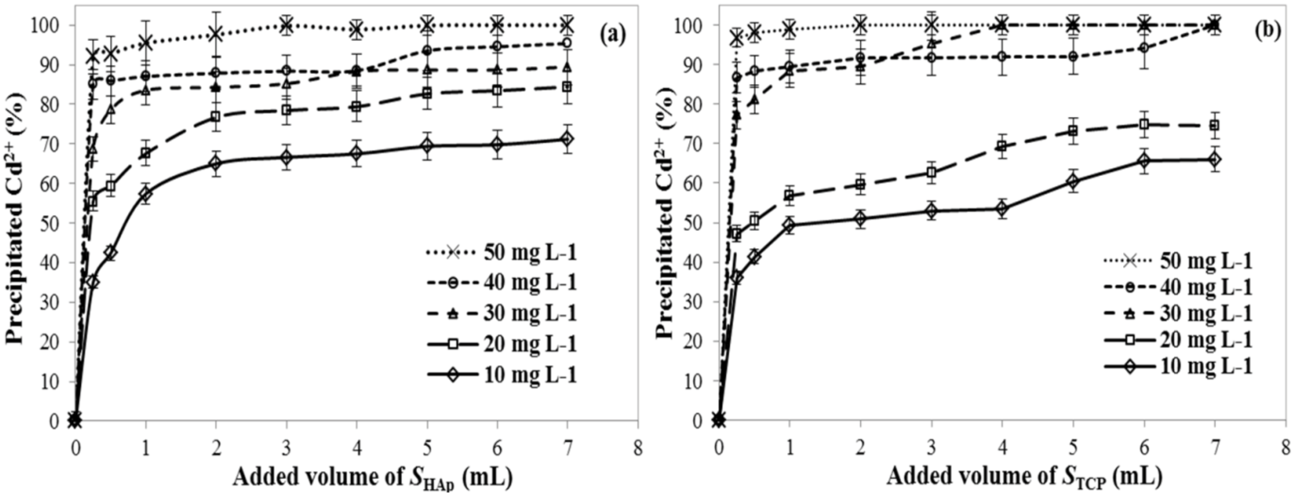

Fig. 2. Efficiency of Cd^{2+} neutralization from solutions with different initial metal concentrations as a function of the added volumes of: (a) S_{HAp} and (b) S_{TCP}.

Table 1
Molar fractions of Cd incorporated per unit cell of the re-precipitated HAp and TCP at pH 7

	HAp				TCP			
C_0 (mg L^{-1})	C_e (mg L^{-1})	V_{add} (mL)	x	Substitution rate (%)	C_e (mg L^{-1})	V_{add} (mL)	x	Substitution rate (%)
10	3.50 ± 0.29	2.00	0.14 ± 0.01	1.45 ± 0.13	5.08 ± 0.38	1.00	0.07 ± 0.01	2.26 ± 0.29
20	4.66 ± 0.35	2.00	0.34 ± 0.02	3.43 ± 0.24	8.65 ± 0.63	1.00	0.16 ± 0.01	5.22 ± 0.54
30	4.93 ± 0.37	1.00	0.12 ± 0.07	11.20 ± 0.69	3.45 ± 0.29	1.00	0.37 ± 0.02	12.21 ± 0.70
40	5.95 ± 0.44	0.25	6.08 ± 0.36	60.86 ± 3.66	5.32 ± 0.39	0.25	1.91 ± 0.11	63.80 ± 3.75
50	3.97 ± 0.31	0.25	8.22 ± 0.45	82.28 ± 4.50	1.60 ± 0.22	0.25	2.67 ± 0.14	89.04 ± 4.62

the conversion rate because more molecules or ions interact to form new compounds [35]. Accordingly, the higher x values at pH 7 were obtained by reacting 50 mg L^{-1} of the Cd^{2+} solution with 0.25 mL of S_{HAp} or S_{TCP}.

3.2. Extending the optimal precipitation conditions to solutions of waste animal bones

3.2.1. Effect of the set precipitation pH

Based on the data reported in Table 1, the optimal conditions (50 mg L^{-1} of Cd^{2+} solution and 0.25 mL of the synthetic phosphate solutions) were selected to investigate the influence of the set precipitation pH, which was varied within the 5-9 range. The experiments performed included all the phosphate-containing solutions derived from synthetic calcium phosphates (S_{HAp} or S_{TCP}) and from acid digestion of the waste animal bones (S_{RBw}, S_{CBw}). The results displayed in Fig. 3 reveal that the novel approach enables achieving comparable degrees of efficiency irrespective of the calcium phosphate source (synthetic or natural). Furthermore, the phosphate solution prepared from rabbit waste bones (S_{RBw}) is more effective in Cd^{2+} neutralization in comparison to its homologous prepared from the chicken bones (S_{CBw}). This difference can be attributed to the higher P-content of rabbit bones in comparison to chicken bones, as determined by EDS. Moreover, the precipitated quantities of Cd^{2+} ions tend to decrease under acid conditions (pH < 7), as expected from the solubility curves of the various calcium phosphate compounds as a function of pH reported elsewhere [36]. Similar results were obtained by adding P-containing solutions prepared from soluble phosphorus compounds such as K_2HPO_4, $NH_4H_2PO_4$, and fertilizer [13].

3.2.2. Kinetic parameters

The kinetics of Cd^{2+} precipitation using phosphate solutions derived from the acid digestion of waste animal bones was evaluated under the optimal conditions determined for the solutions prepared from the synthetic calcium phosphates. Hence, 0.25 mL of each S_{Hap} and S_{TCP} solution was added to 50 mg L^{-1} of the synthetic waste water at pH 7. Fig. 4 shows that whatever is the type of the added solution, the equilibrium extraction of Cd^{2+} from water was rapidly established. The kinetic parameters were determined though the application of the pseudo-second-order kinetic model which is related to the chemical bonding reactions [37], which could be described by the following equation:

$$\frac{t}{x_t} = \frac{1}{kx_e^2} + \frac{1}{x_e}t \tag{9}$$

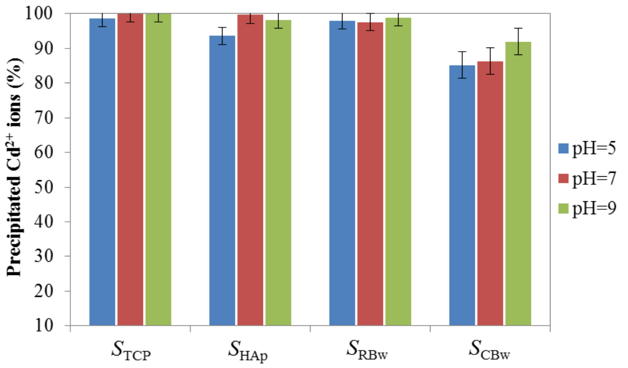

Fig. 3. Efficiency in Cd^{2+} precipitation by adding the investigated phosphate solutions S_{HAp}, S_{TCP}, S_{RBw}, and S_{CBw}, under the following experimental conditions: $[Cd^{2+}]_0$ = 50 mg L^{-1}; V_{Cd} = 100 mL; V_{add} = 0.25 mL; pH = 5, 7, and 9).

where x_t and x_e are the quantities of the metal ion precipitated at a given reaction time t, and the equilibrium extraction, respectively (in a mole of Cd^{2+} ions per mole of Ca-Cd-phosphate apatite), and k is the pseudo-second-order constant of the reaction $[mol_{apatite} (mol_{Cd} min)^{-1}]$. From the plot of t/x_t vs. t inserted in Fig. 4, the slope and the intercept of the straight lines led to the theoretical values of x_e and k parameters, respectively. The related relevant data gathered in Table 2 show good coincidences between the experimental and the calculated x_e values for the three tested cases. Furthermore, it can be concluded that irrespective of the phosphate source, natural or synthetic apatite, the solutions derived thereof exhibit similar performances in Cd^{2+} precipitation from contaminated waters.

3.2.3. Applicability of the method to higher metal concentrations

The robustness of the proposed method to neutralize aqueous cadmium was further tested using metal concentrations within the range of 100-500 mg L^{-1}, while the mass ratio of the aqueous cadmium to the added dissolved apatite phosphate was kept constant. However, the reaction time has been limited to 15 min. From Fig. 5, it can be seen that the percentage of aqueous Cd^{2+} precipitated is almost constant for S_{RBw} addition (~99%), being slight lower (~97%) for S_{CBw} addition.

3.2.4. Effect of coexisting heavy metals

Considering that several heavy metals often coexist in wastewaters, and the difficulty in obtaining a real wastewater sample in our country, the efficiency of the precipitation process in neutralizing heavy metals was also investigated in a multi-component system. Therefore, a synthetic wastewater sample containing 50 mg L^{-1} of each Cd^{2+}, Pb^{2+}, Zn^{2+}, Fe^{2+}, and Cu^{2+}, totalizing an overall concentration $[M^{2+}]_0$ of 250 mg L^{-1} was prepared for this purpose. The results are shown in Fig. 6. It could be noticed that the other coexisting cations in the solution had no great impact on the removal percentage of Cd^{2+}. Furthermore, this technique could successfully be applied to neutralize heavy metals in wastewaters.

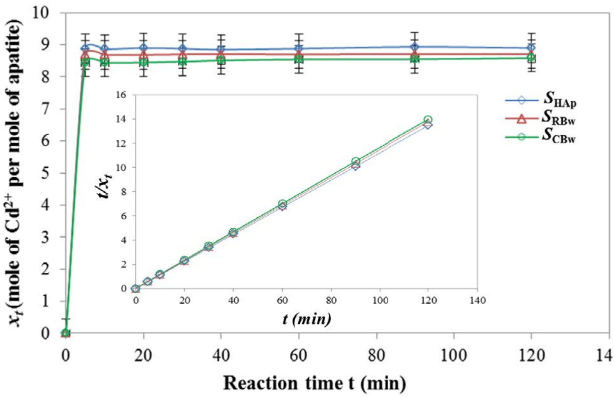

Fig. 4. Application of the pseudo-second-order kinetic model to the experimental results of Cd^{2+} precipitation using phosphate solutions prepared from the natural apatites (S_{RBw}, S_{CBw}) and from the synthetic hydroxyapatite apatite (S_{HAp}) under the following experimental conditions: $[Cd^{2+}]_0$ = 50 mg L^{-1}; V_{Cd} = 100 mL; V_{add} = 0.25 mL; pH = 7.

Table 2
Kinetic parameters of Cd^{2+} precipitation upon adding three types of the phosphate solutions (S_{HAp}, S_{RBw}, and S_{CBw})

Phosphate solution	Kinetic parameters			
	$x_{e,exp}$	$x_{e,cal}$	k	R^2
S_{HAp}	8.888	8.913	1.593	1
S_{RBw}	8.700	8.711	4.881	1
S_{CBw}	8.501	8.591	0.529	1

3.3. Identification of the metal-forming phosphates

3.3.1. FTIR and XRD analysis of natural and Cd-containing re-precipitated apatites

FTIR and XRD analysis were performed for the starting powdered bones (RBw and CBw) and for the re-precipitated apatite powders, RBw-Cd and CBw-Cd, derived thereof by adding their acid digestion solutions to Cd-containing synthetic wastewater. The main aims were: (i) determining the functional groups and the crystalline phase assemblages in both types of apatites; (ii) check if the Cd-neutralizing process brings any functional or structural changes.

The recorded FTIR spectra depicted in Fig. 7a exhibit the characteristic absorbance bands of PO_4^{3-} group appearing at 560; 601; 969; 1,017 cm^{-1} for rabbit derived samples, RBw and RBw-Cd. Similar but less discretized vibration bands appear centered at 560 and 1,000 cm^{-1} for the chicken derived CBw and CBw-Cd (Fig. 7b). The spectra also reveal low-intensity peaks at ~3,570 and sharpener ones at ~1,660 cm^{-1}, which are assigned to structural OH^- groups and N–H bands, respectively. Besides, the bands located at 875 cm^{-1} and those in the region of 1,420–1,570 indicate the presence of CO_3^{2-} groups partially substituting the PO_4^{3-} tetrahedrons. This means that all the samples can be identified as B-type carbonate apatites [38,39]. The XRD patterns displayed in Figs. 7c and d are typical of apatites with low crystallinity, especially for the chicken derived

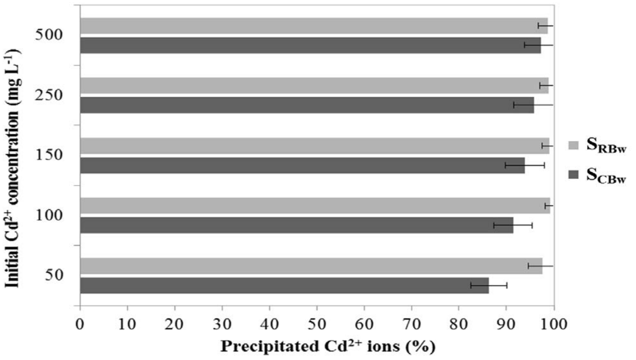

Fig. 5. Precipitated Cd^{2+} ions in water for different initial concentrations using the corresponding quantities of the phosphate solutions S_{RBw} and S_{CBw} under the following experimental conditions: pH = 7; reaction time = 15 min.

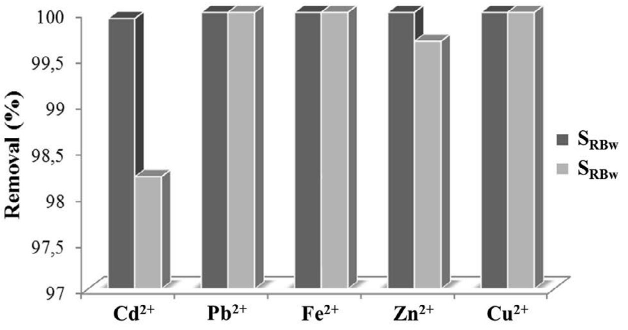

Fig. 6. Efficiency of the precipitation process in neutralizing Cd^{2+}, Pb^{2+}, Fe^{2+}, Zn^{2+}, and Cu^{2+} in a synthetic wastewater sample under the following experimental conditions: $[M^{2+}]_0 = 250$ mg L^{-1}; $V_{Cd} = 100$ mL; $V_{add} = 1.25$ mL; pH = 7.

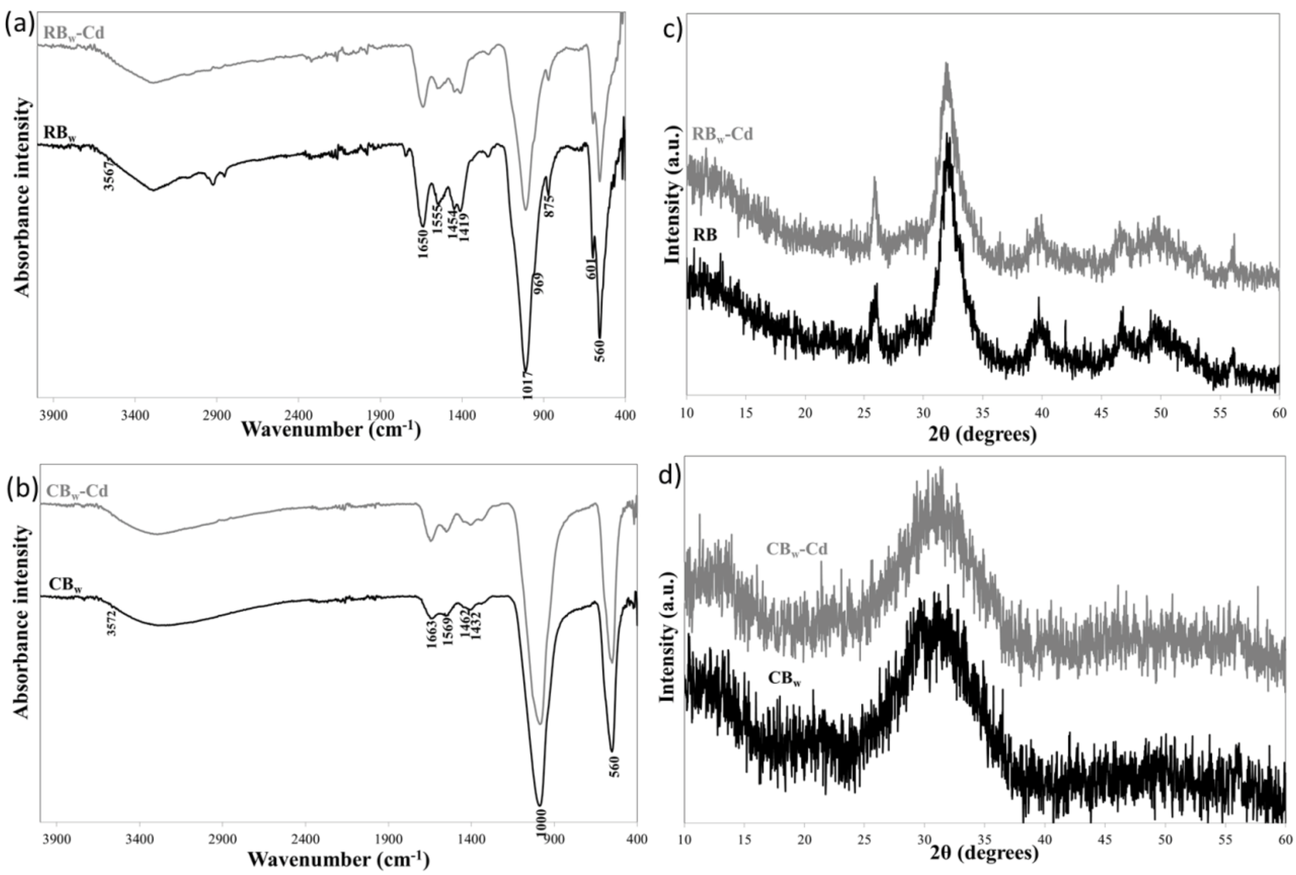

Fig. 7. FTIR spectra (a and b) and XRD patterns (c and d) of powdered rabbit and chicken bones (RBw, CBw) and the respective Cd-containing precipitates (RBw-Cd, CBw-Cd) derived thereof, following the novel approach here proposed for removing aqueous cadmium from wastewaters.

samples, as deduced from the broad and low-intensity peaks. This is in good agreement with similar observations reported elsewhere [40]. The difference between the rabbit- and chicken-derived samples is likely attributable to the lower P-content measured by EDS for the chicken bones. However, structural differences between the original powdered bones and the respective Cd-containing precipitates can hardly be distinguished.

The similarity in the recorded spectra for these products and those of the starting minerals indicates that the re-precipitation process does not contribute to any apparent functional or structural modifications.

3.3.2. SEM-EDS analysis

Fig. 8 compares the EDS spectra and the morphological features (inserted SEM images) of the powdered rabbit and chicken bones (RBw, CBw) with those of the respective Cd-containing precipitates (RBw-Cd, CBw-Cd). The SEM images reveal that the re-precipitation process induced some morphological changes. But the most salient feature is the clear cadmium enrichment of the precipitated solids well evidenced in the displayed EDS spectra.

The atomic contents deduced from the EDS peak integration are displayed in Fig. 9, and the corresponding compositions are reported in Table 3. The chemical formulas of the starting minerals and the final precipitates given in Table 3, were determined considering the general chemical formula proposed for the carbonate-containing apatites $Ca_{10-x}(PO_4)_{6-x}(CO_3)_x(OH)_{2-x}$ (with $0 \leq x \leq 2$) on the one hand [41], and the coexistence of trace elements of Mg^{2+}, Na^{+}, and Al^{3+} in the cationic sites, on the one other hand. Accordingly, the molar ratios of the total metal ions to phosphate (M/PO_4^{3-}) for the starting minerals are around 1.8. This slight deviation from the stoichiometric value of the pure HAp (1.67) has been already reported by mineralogist studies [42]. It was explained by the coexistence of minor fractions of tricalcium phosphate $Ca_3(PO_4)_2$ and tetracalcium phosphate $Ca_4P_2O_9$ in the biologic apatite [30]. Otherwise, it may be the consequence of CO_3^{2-} groups partially substituting PO_4^{3-} in the B-sites [38].

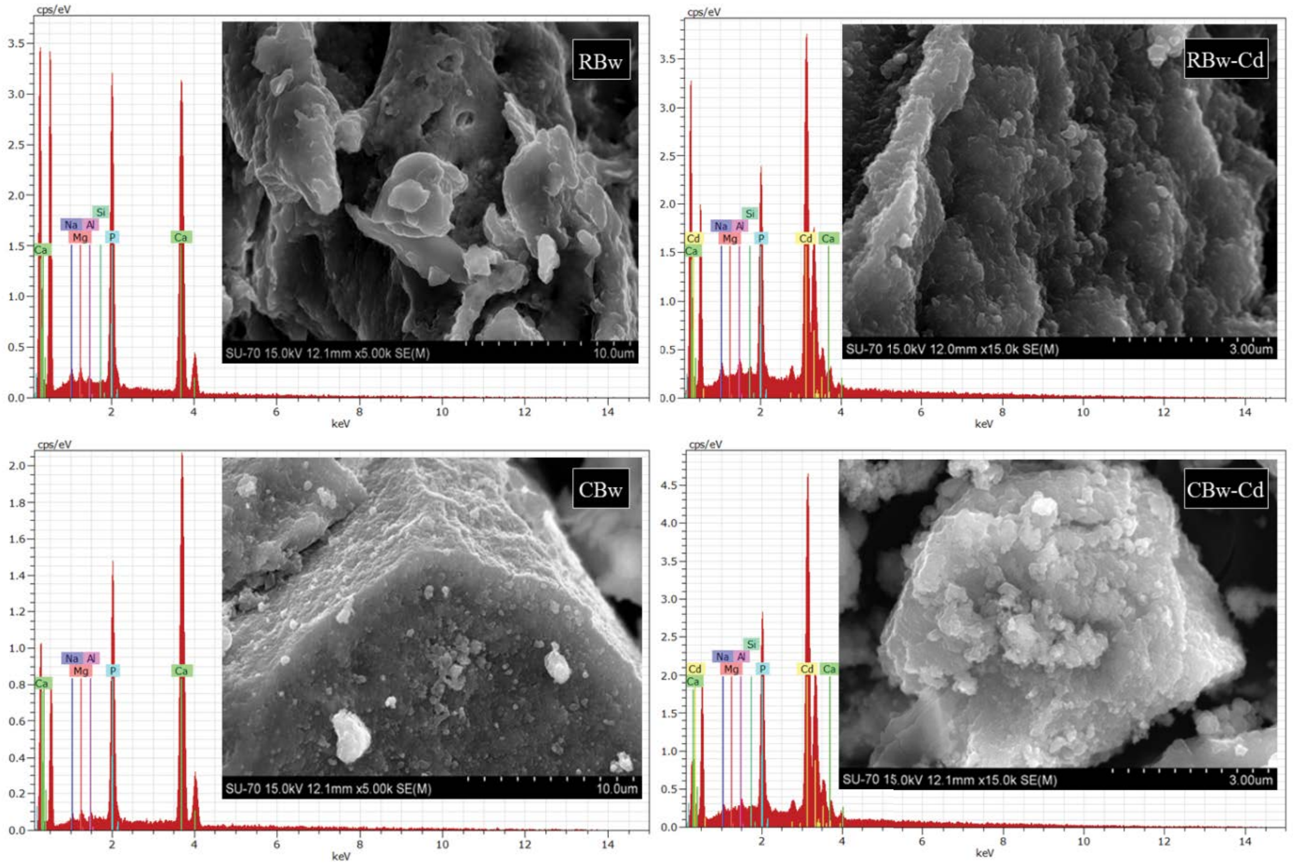

Fig. 8. EDS spectra (SEM images inserted) of the waste animal bones before (RBw, CBw, on the left side) and after being re-precipitated in Cd-loaded solutions (RBw-Cd, CBw-Cd, on the right side).

Table 3
Chemical formula of the waste animal bones before and after being re-precipitated in Cd-loaded solutions together with the corresponding (M/PO_4^{3-}) molar ratio

Sample	Chemical formula	M/PO_4^{3-}
RBw	$Ca_{9.62}Mg_{0.14}Na_{0.19}Al_{0.04}(PO_4)_{5.62}(CO_3)_{0.38}(OH)_{1.62}$	1.78
RBw-Cd	$Ca_{0.39}Cd_{8.33}Mg_{0.11}Na_{0.74}Al_{0.42}(PO_4)_{4.33}(CO_3)_{1.67}(OH)_{0.33}$	2.31
CBw	$Ca_{9.42}Mg_{0.25}Na_{0.23}Al_{0.10}(PO_4)_{5.42}(CO_3)_{0.58}(OH)_{1.42}$	1.84
CBw-Cd	$Ca_{0.19}Cd_{9.19}Mg_{0.00}Na_{0.42}Al_{0.20}(PO_4)_{5.19}(CO_3)_{0.81}(OH)_{1.19}$	1.93

The overall data collected in the frame of this work are highly meaningful, enabling to deduce that ~87% of the cationic sites in the re-precipitated Ca-Cd-phosphate apatites are occupied by Cd^{2+} ions. These results are in agreement with those of the liquid analysis. Furthermore, the trapped quantity of cadmium according to this method ($x_e \approx 8.7$) is significantly higher in comparison to the adsorbed amount of the metal ion onto the bone-derived apatite through the batch equilibrium process ($x_e \approx 1.0$) [43].

4. Conclusion

Waste animal bones were successfully exploited as sources of PO_4^{3-} ions to precipitate aqueous cadmium from wastewaters. Based on FTIR, XRD, and EDS analyses, the novel cadmium neutralization approach leads to the formation at pH 7 of $Ca_{(10-x)}$-Cd_x-phosphate apatites with a Cd atomic fraction, $x = 0.87$, therefore, about nine times higher than the cadmium removal contents usually trapped by the bone-derived apatite through the adsorption processes.

The equilibrium extraction was well-described by the pseudo-second-order kinetic model which is related to the chemical bonding reactions. Accordingly, the calculated x_e values were in a good agreement with the experimental data. Furthermore, the efficiency of the precipitation process in neutralizing Cd^{2+} has been evinced for single and multi-component systems, conferring to the proposed novel approach good prospects in terms of applicability for cleaning real wastewaters.

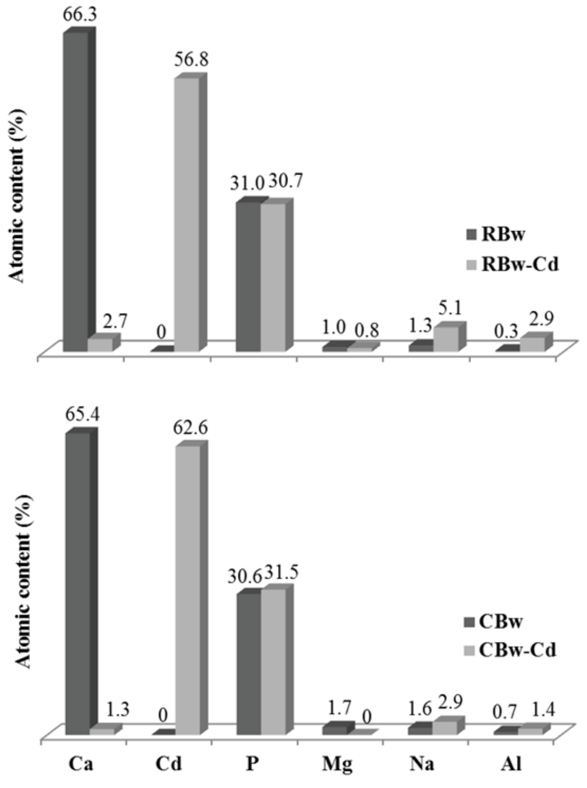

Fig. 9. Elemental composition of the final precipitates compared to that of the starting waste animal bones.

This low-cost remediation technique is a promising alternative to convert high levels of cadmium and other pollutants in wastewater into stable edifices of metal-phosphate apatites. Moreover, considering that the required doses of phosphates are much lower, the expected volume of the resulting sludges can be significantly reduced in comparison to those generated by the traditional adsorption-based processes.

Acknowledgments

The authors are grateful to Professor J.M.F. Ferreira, from University of Aveiro Portugal, Department of Materials and Ceramics Engineering, CICECO-Aveiro Institute of Materials, for SEM-EDS analyses and for English editing and review.

References

[1] D.C. Adriano, Trace Elements in Terrestrial Environments: Biogeochemistry, Bioavailability and Risks of Metals, 2nd ed., Springer-Verlag, New York, NY, 2001.

[2] M. Hutton, Sources of cadmium in the environment, Ecotoxicol. Environ. Saf., 7 (1983) 9–24.

[3] R.D. Davis, Cadmium-A complex environmental problem part II: cadmium in sludges used as fertilizer, Experientia, 40 (1984) 117–126.

[4] L. Jarup, L. Hellstrom, T. Alfven, M. Carlsson, A. Grubb, B. Persson, C. Pettersson, G. Spang, A. Schutz, C. Elinder, Low level exposure to cadmium and early kidney damage: the OSCAR study, J. Occup. Environ. Med., 57 (2000) 668–672.

[5] M. Fleischer, A.F. Sarofim, D.W. Fassett, P. Hammond, H.T. Shacklette, I.C. Nisbet, S. Epstein, Environmental impact of cadmium: a review by the panel on hazardous trace substances, Environ. Health Perspect., 7 (1974) 253–323.

[6] P. Elliott, R. Arnold, S. Coching, N. Eaton, L. Jarup, J. Jones, M. Quinn, M. Rosato, I. Thornton, M. Toledano, E. Tristan, J. Wakefield, Risk of mortality, cancer incidence, and stroke in a population potentially exposed to cadmium, Occup. Environ. Med., 57 (2000) 94–97.

[7] M. Nishijo, H. Nakagawa, Y. Suwazono, K. Nogawa, T. Kido, Causes of death in patients with Itai–itai disease suffering from severe chronic cadmium poisoning: a nested case-control analysis of a follow-up study in Japan, BMJ Open, 7 (2017) 1–7, doi: 10.1136/bmjopen-2016–015694.

[8] P.M. Ferraro, S. Costanzi, A. Naticchia, A. Sturniolo, G. Gambaro, Low level exposure to cadmium increases the risk of chronic kidney disease: analysis of the NHANES 1999–2006, BMC Public Health, 10 (2010) 1–8, doi: 10.1186/1471-2458-10-304.

[9] H. Liu, W. Xia, S. Xu, B. Zhang, B. Lu, Z. Huang, H. Zhang, Y. Jian, W. Liu, Y. Peng, X. Sun, Y. Li, Cadmium body burden and pregnancy-induced hypertension, Int. J. Hyg. Environ. Health, 221 (2018) 246–251.

[10] A. Engstom, K. Michaelsson, M. Vahter, B. Julin, A. Wolk, A. Akesson, Associations between dietary cadmium exposure and bone mineral density and risk of osteoporosis and fractures among women, Bone, 50 (2012) 1372–1378.

[11] J.A. McElroy, M.M. Shafer, A. Trentham-Dietz, J.M. Hampton, P.A. Newcomb, Cadmium exposure and breast cancer risk, J. Natl. Cancer Inst., 98 (2006) 869–873.

[12] J.K. Song, H. Luo, X.H. Yin, G.L. Huang, S.Y. Luo, D. Lin, J. Zhu, Association between cadmium exposure and renal cancer risk: a meta-analysis of observational studies, Sci. Rep., 5 (2015) 1–8.

[13] J. Mastusik, T. Bajda, M. Manecki, Immobilization of aqueous cadmium by addition of phosphates, J. Hazard. Mater., 152 (2008) 1332–1339.

[14] Z. Zang, J. Ren, M. Young, X. Song, C. Zhang, J. Chen, F. Li, G. Guo, Competitive immobilization of Pb in an aqueous

ternary-metals system by soluble phosphates with varying pH, Chemosphere, 159 (2016) 58–65.

[15] J. Kheriji, D. Tabassi, B. Hamrouni, Removal of Cd(II) ions from aqueous solution and industrial effluent using reverse osmosis and nanofiltration membranes, Water Sci. Technol., 72 (2015) 1206–1216.

[16] C.W. Wong, J.P Barford, G. Chen, G. McKay, Kinetics and equilibrium studies for the removal of cadmium ions by ion exchange resin, J. Environ. Chem. Eng., 2 (2014) 698–707.

[17] S.Y. Kim, M.R. Jin, C.H. Chung, Y.S. Yun, K.Y. Jahng, K.Y. Yu, Biosorption of cationic basic dye and cadmium by the novel biosorbent *Bacillus catenulatus* JB-022 strain, J. Biosci. Bioeng., 119 (2014) 433–439.

[18] F.A. Al-Khaldi, B. Abu-Sharkh, A.M. Abulkibash, M.A. Atieh, Cadmium removal by activated carbon, carbon nanotubes, carbon nanofibers, and carbon fly ash: a comparative study, Desal. Water Treat., 53 (2013) 1–13.

[19] D. Wang, X. Guan, F. Huang, S. Li, Y. Shen, J. Chen, H. Long, Removal of heavy metal ions by biogenic hydroxyapatite: morphology influence and mechanism study, Russ. J. Phys. Chem., 90 (2016) 1557–1562.

[20] A. Dybowska, D.A.C. Manning, M.J. Collins, T. Wess, S. Woodgate, E. Valsami-Jones, An evaluation of the reactivity of synthetic and natural apatites in the presence of aqueous metals, Sci. Total Environ., 407 (2009) 2953–2965.

[21] S. Kannan, F.G. Neunhoeffer, J. Neubauer, S. Pina, P.M.C. Torres, J.M.F. Ferreira, Synthesis and structural characterization of strontium- and magnesium-co-substituted β-tricalcium phosphate, Acta Biomater., 6 (2010) 571–576.

[22] S. Pina, P.M. Torres, F.G. Neunhoeffer, J. Neubauer, J.M.F. Ferreira, Newly developed Sr-substituted α-TCP bone cements, Acta Biomater., 6 (2010) 928–935.

[23] S. Kannan, F.G. Neunhoeffer, J. Neubauer, J.M.F. Ferreira, Cosubstitution of zinc and strontium in β-tricalcium phosphate: synthesis and characterization, J. Am. Ceram. Soc., 94 (2010) 230–235.

[24] S. Kannan, F.G. Neunhoeffer, J. Neubauer, A.H.S. Rebelo, P. Valério, J.M.F. Ferreira, Rietveld structure and *in vitro* analysis on the influence of magnesium in biphasic (hydroxyapatite and β-tricalcium phosphate) mixtures, J. Biomed. Mater. Res. Part B, 90 (2008) 404–411.

[25] A.S. Neto, A.C. Fonseca, J.C.C. Abrantes, J.F.J. Coelho, J.M.F. Ferreira, Surface functionalization of cuttlefish bone-derived biphasic calcium phosphate scaffolds with polymeric coatings, Mater. Sci. Eng., C, 105 (2019) 1–41, doi: 10.1016/j.msec.2019.110014.

[26] S. Kannan, F.G. Neunhoeffer, J. Neubauer, J.M.F. Ferreira, Ionic substitutions in biphasic hydroxyapatite and β-tricalcium phosphate mixtures: structural analysis by rietveld refinement, J. Am. Ceram. Soc., 91 (2008) 1–12.

[27] A.H.S. Rebelo, J.M.F. Ferreira, Comparison of cadmium removal efficiency by two calcium phosphate powders, J. Environ. Chem. Eng., 5 (2017) 1475–1483.

[28] R. Aouay, S. Jebri, A. Rebelo, J.M.F. Ferreira, I. Khattech, Enhanced cadmium removal from water by hydroxyapatite subjected to different thermal treatments, J. Water Supply Res. Technol. AQUA, 69 (2020) 678–693.

[29] D. Marchat, D. Bernache-Assollant, E. Champion, Cadmium fixation by synthetic hydroxyapatite in aqueous solution – thermal behaviour, J. Hazard. Mater., 139 (2007) 453–460.

[30] G.S. Johnson, M.R. Mucalo, M.A. Lorier, U. Gieland, H. Mucha, The processing and characterization of animal-derived bone to yield materials with biomedical applications. Part II: milled bone powders, reprecipitated hydroxyapatite and the potential uses of these materials, J. Mater. Sci.: Mater. Med., 11 (2000) 725–741.

[31] S. Jebri, I. Khattech, M. Jemal, Standard enthalpy, entropy and Gibbs free energy of formation of ˝A” type carbonate phosphocalcium hydroxyapatites, J. Chem. Thermodyn., 106 (2017) 84–94.

[32] S. Ben Abdelkader, A. Ben Cherifa, I. Khattech, M. Jemal, Synthesis, characterization and thermochemistry of tri-magnesium phosphate and tri-calcium phosphate, Thermochim. Acta, 334 (1999) 123–129.

[33] A. Ben Cherifa, M. Jemal, Enthalpy of formation and mixing of calcium-cadmium phosphoapatites, Phosphorus Res. Bull., 15 (2004) 113–118.

[34] A. Ben Cherifa, M. Jemal, Synthèse et thermochimie de phosphates au cadmium Partie I: Cas du phosphate tricadmique et de la chlorapatite cadmiée, Thermochim. Acta, 366 (2001) 1–6.

[35] R. Myers, The Basics of Chemistry: Basics of the Hard Sciences, Greenwood Press, Westport, Ireland, 2003.

[36] K. Ishikawa, Bone substitute fabrication based on dissolution-precipitation reactions, Materials, 3 (2010) 1138–1155.

[37] Y.S. Ho, Review of second-order models for adsorption systems, J. Hazard. Mater., 136 (2006) 681–689.

[38] H. Madupalli, B. Pavan, M.M.J. Tecklenburg, Carbonate substitution in the mineral component of bone: discriminating the structural changes, simultaneously imposed by carbonate in A and B sites of apatite, J. Solid State Chem., 255 (2017) 27–35.

[39] S.L. Bee, Z.A. Abdul Hamid, Characterization of chicken bone waste-derived hydroxyapatite and its functionality on chitosan membrane for guided bone regeneration, Compos. Part B: Eng., 163 (2019) 562–573.

[40] L.C. Bonar, A.H. Roufosse, W.K. Sabine, M.D. Grynpas, M.J. Glimcher, X-ray diffraction studies of the crystallinity of bone mineral in newly synthesized and density fractionated bone, Calcif. Tissue Int., 35 (1983) 202–209.

[41] J.C. Labarthe, G. Bonel, G. Montel, Structure and properties of B-type phosphocalcium carbonate apatites, Ann. Chim., 8 (1973) 289–301.

[42] N. Kourkoumelis, I. Balatsoukas, M. Tzaphlidou, Ca/P concentration ratio at different sites of normal and osteoporotic rabbit bones evaluated by Auger and energy dispersive X-ray spectroscopy, J. Biol. Phys., 38 (2011) 279–291.

[43] E.A. Ofudje, I.A. Adeogun, M. Idowu, Simultaneous removals of cadmium(II) ions and reactive yellow 4 dye from aqueous solution by bone meal-derived apatite: kinetics, equilibrium and thermodynamic evaluations, J. Anal. Sci. Technol., 11 (2020) 1–16.